Journal of GeoEngineering, Vol. 11, No. 3, pp. 133-142, December 2016
http://dx.doi.org/10.6310/jog.2016.11(3).3

EVALUATION OF SIZE AND BOUNDARY EFFECTS IN SIMPLE SHEAR TESTS WITH DISTINCT ELEMENT MODELING

Wen-Jong Chang [1], Thitibhorn Phantachang [2*], and Wai-Man Ieong [3]

ABSTRACT

Because the direct simple shear (DSS) mode is recognized as the most representative failure condition along a sliding surface, a DSS testing system capable of testing large soil particles is useful to determine the strength parameters of gravelly soils. In DSS tests, the size and boundary effects are two crucial factors that affect the consistency of the test results. To evaluate the size and boundary effects in DSS conditions, numerical experiments using the distinct element method are performed to investigate the influences of specimen dimensions on the macroscopic stress-strain relationship and microscopic uniformity in terms of the specimen diameter (D), specimen height (H), and maximum particle size (d_{max}). The size effect is evaluated on the variations of stress-strain curves with the specimen dimensions and d_{max}. The boundary effect is assessed in terms of the spatial distribution of the particle displacement and contact force fields. The results show that: 1. the boundary effect can be reduced effectively when H/D decreases, 2. the difference in boundary effect is insignificant between Cambridge and Norwegian Geotechnical Institute types of simple shear configurations, and 3. there is a relatively consistent stress-strain relationship when H/d_{max} is no less than 7.

Key words: Simple shear test, size effect, boundary effect, distinct element method.

1. INTRODUCTION

Slope failures in colluvium strata triggered by rainfall are frequently reported in mountainous areas. Strength parameters and the stress-strain relationship are essential for evaluating the slope stability of colluvium. Depending on the composition of materials and degree of coherence, colluvium can be categorized as rock or soil mass, the latter of which is more vulnerable to slope failure. For soil-like colluvium, which is composed of a matrix of soil particles mixed with rock fragments or gravel, the incoherence of colluvium allows colluvial deposits to be treated as granular materials. Soils with gravel particles are generally called gravelly soils, which include colluvium, rockfill, and tailings. Limited by the available testing apparatus and sample reconstitution procedure, representative strength parameters and the stress-strain relationship are difficult to determine in gravelly soils due to the existence of large particles and the complexity of the grain size distribution. To tackle these issues, a research project is conducted with hybrid numerical and physical element tests of steel balls to represent idealized granular assembles. Because the direct simple shear (DSS) mode is recognized as the most representative failure condition along a sliding surface, a DSS testing system capable of testing gravelly soils with large soil particles is developed in the present study.

DSS tests have been used by researchers to evaluate the soil properties and stress-strain responses of soils under simple shear straining mode, which can represent soil conditions in slope stability analyses, foundation and embankment designs, and seismic analysis. In these applications, soil elements are consolidated and sheared under the Ko condition with zero horizontal deformation. The strength anisotropy from the rotation of principle stresses during shearing can be mitigated with DSS strength parameters (Ladd and Foott 1974) and the results are close to those from vane shear and back analyses (Airey and Wood 1987).

In DSS tests, the size and boundary effects are two crucial factors affecting the consistency of the test results. To quantitatively evaluate the size and boundary effects in simple shear conditions, numerical experiments using the distinct element method (DEM) are conducted in the present study and validated by physical element tests on uniform steel balls using a simple shear apparatus. The validated models are used to investigate the influences of specimen dimensions and maximum particle size on macroscopic stress-strain responses and microscopic uniformity on particle force and displacement fields.

1.1 Boundary and Size Effects in Direct Simple Shear Test

In physical element tests, soil specimens are tested under stress/strain boundary constrains that mimic field conditions. In a continua framework, boundary effects refer to the non-uniformity of stress near the specimen boundaries and size effects refer to the variation of shear strength due to specimen size. To find representative and consistent results, the boundary and size effects need to be clarified.

Two types of DSS device, developed by the Norwegian Geotechnical Institute (NGI) and Cambridge University, abbreviated as NGI-DSS and CAM-DSS, respectively, have been developed. The major difference between them is the type of soil container. The NGI-DSS developed by Bjerrum and Landva (1966) is a modified design of Kjellman (1951) with a wire-reinforced

Manuscript received March 9, 2016; revised June 30, 2016; accepted July 1, 2016.
[1] Associate Professor, Department of Civil Engineering, National Cheng Kung University, 1 University Road, Tainan, Taiwan.
[2] Graduate Student (corresponding author), Graduate Research Assistant, Department of Civil Engineering, National Cheng Kung University (e-mail: rockmass@gmail.com).
[3] Engineer, Taipei Geotechnical Department, Resources Engineering Services Inc..

rubber membrane to confine a cylindrical soil sample and maintain the Ko condition throughout the test. CAM-DSS (Roscoe 1953) utilizes a cuboidal sample mounted on a rigid steel plate and rotated by two hinged end flaps. Due to the lack of control of the complimentary shear stresses on the vertical sides, the non-uniformity of the stress field within the specimen is a major concern in promoting DSS testing in geotechnical profession.

Numerous experimental studies (*e.g.*, Wright *et al.* 1978; Airey and Wood 1987; Budhu 1984; Kishida and Uesugi 1987) and analytical works (*e.g.*, Lucks *et al.* 1972; Prevost and Hoeg 1976; Budhu and Britto 1987; Dounias and Potts 1993; Doherty and Fahey 2011) have been conducted to assess the effects of non-uniform stress fields within DSS specimens. All of these studies concluded that the non-uniform stress conditions within the specimen are induced by the incomplete mobilization of shear stress along the side walls of specimens. However, Roscoe (1953) stated that the stress distributions within the core of specimens were uniform and the testing results of Airey and Wood (1987) for clay with an NGI-DSS system confirmed this finding. Lucks *et al.* (1972) performed three-dimensional (3D) finite element analysis on the NGI-DSS configuration and showed that the stress concentration only occurred within the proximity of the specimen boundaries and that around 70% of the specimen was subjected to a uniform stress field.

In simple shear conditions, the boundary effect mainly depends on the specimen height (H) to diameter (D) ratio (H/D). Based on 3D finite element analysis results, Shen *et al*. (1978) concluded that the deviation of the induced shear strains near the specimen boundaries decreased with decreasing H/D ratio. Amer *et al.* (1987) showed that the difference of shear stress near the boundaries is 30% of the value in the core zone. In summary, the boundary effects in DSS configurations are closely related to the H/D ratio.

The major factors that affect the shear strength of soils are the maximum particle size (d_{max}), particle shape, grain size distribution, stress state, and straining mode. In laboratory element tests, the measured shear strength was affected by the specimen size (Amer *et al*. 1987). For DSS tests on gravelly soils, the size effects control the specimen size, which is crucial for designing the DSS apparatus. In this study, idealized granular systems are analyzed under DSS conditions using DEM. The boundaries and specimen size effects on DSS conditions with idealized round particles are studied to determine the optimal specimen configurations for testing real colluvium.

1.2 Distinct Element Method

Cundall and Strack (1979) used DEM to simulate granular systems by representing the discontinuous nature of granular materials by a set of discrete elements. Since then, several DEM codes had been developed to simulate particle responses in various professions (Kozicki and Donze 2008). The DEM code used in this study is the Particle Flow Code in Two Dimensions (PFC^{2D}) by Itasca Inc. (2008) based on works by Cundall and Strack (1979). This program models two-dimensional (2D) assemblies of rigid discs. An explicit numerical scheme is employed in PFC^{2D} to solve Newton's second law for the particle assembly with a force-displacement law applied at the contact points and update the contact conditions arising from the relative motion of particles.

Numerous studies have been conducted to study granular material response (Thornton 2000; Cui and O'Sullivan 2006; Zhao and Evans 2009; Wang and Gutierrez 2010). There have been few attempts to simulate the DSS test using DEM. Wijewickreme *et al*. (2013) conducted a drained and constant-volume DSS simulation using 3D DEM to examine the mobilized friction angle. Dabeet *et al.* (2015) perform a 3D DEM simulation on simple shear test to investigate stress-strain nonuniformity. Their results showed that mobilised stress ratio distribution at the central planes is uniform. These studies showed the potential of using DEM to evaluate the soil behaviors under DSS shearing. However, these studies did not consider the spatial variations of microscopic responses and the effects of specimen size and boundary conditions.

The objective of this study is to examine the responses of idealized particle systems using both laboratory experiments and DEM simulations. Modeling details, parametric studies and distributions of particle responses in the DSS models are presented. Quantitative dimensional criteria for DSS specimens are proposed based on the hybrid studies.

2. DIRECT SIMPLE SHEAR TESTING

2.1 Testing Apparatus and Sample Preparation

A modified NGI-type DSS apparatus was used to perform laboratory experiments of idealized particle assemblies. The DSS system was developed at National Cheng Kung University (NCKU-DSS) and is capable of applying monotonic and cyclic loadings for both stress- and strain-controlled conditions in vertical and horizontal directions using two close-looped direct-drive motors (Fig. 1). A soil container (Fig. 1(b)) with a conventional latex membrane reinforced with low-friction stack rings is used in the NCKU-DSS system to maintain the Ko condition throughout testing. Details of the stack-ring-reinforced membrane can be found in Chang *et al*. (2014). The setup of NCKU-DSS with a specimen is shown in Fig. 1(a). In this study the specimen diameter was 100 mm and the height was varied from 20 to 35 mm.

To provide verification data for DEM model, dry, smooth steel balls for ball bearings with a diameter of 1.5 mm were used to fill the soil container and sheared under a constant vertical stress with a fixed displacement rate of 0.1 mm/hr. To reduce the variation of packing during sample preparation, the steel balls were placed in the DSS container in ten layers and the void ratio was controlled to the dense-packed condition by shaking the bottom part of the DSS specimen. The prepared specimen is shown in Fig. 2.

2.2 Experimental Program and Results

In this study, a hybrid technique that involves both physical testing and numerical simulations is adopted. The physical DSS testing on uniform steel balls provided data for calibrating the input parameters and validation cases for DEM simulations for size and boundary effects. For physical DSS testing, steel balls with a diameter of 1.5 mm were employed to prepare the densest packing specimens with a diameter of 100 mm and heights of 20, 30, and 35 mm to represent H/D ratios of 0.20, 0.30, and 0.35, respectively. The void ratio for steel ball specimens is about 0.35. For each H/D ratio, three specimens were prepared and sheared under vertical stresses of 100, 150, and 300 kPa. The results are shown in Fig. 3.

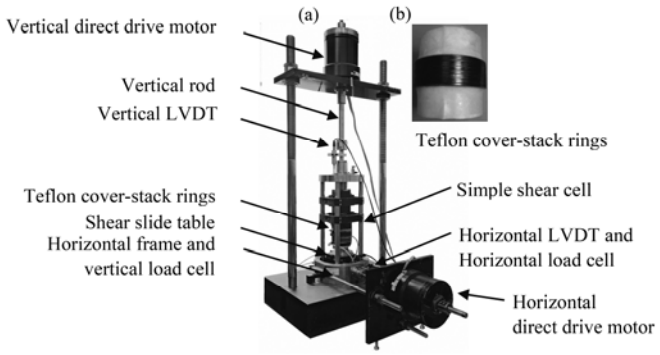

Fig. 1 Details of (a) NCKU-DSS system and (b) soil container

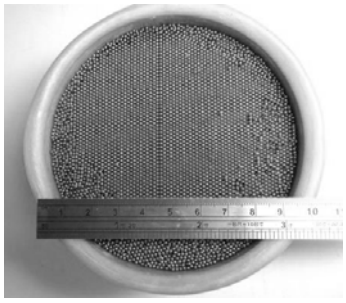

Fig. 2 Uniform steel ball specimen for DSS testing

Figures 3(a) ~ 3(c) present the stress-strain and volumetric strain curves up to 10% of the shear strain for H/D ratios of 0.20, 0.30, and 0.35, respectively. The shear stress-strain curves for all specimens show typical loose-packed responses such as a monotonic increase in shear stress with shear strain level and an increase of contractive volumetric strain with increasing vertical effectives stress. The Mohr-Coulomb failure envelopes with failure occurring at 10% of the shear strain are plotted in Fig. 3(d). The friction angles of uniform steel balls at the densest packing are 17.2°, 18.7°, and 15.9° for H/D ratios of 0.20, 0.30, and 0.35, respectively. These values are much smaller than those of real granular soils due to the uniform size, round shape, and smooth surface of the steel balls.

3. DEM SIMULATION

3.1 Model Details

To take advantage of the axisymmetry of cyclical specimens, a 2D simulation was adopted. The DEM code used in this study is PFC^{2D}, which models particles as rigid circular discs. To verify the simulation with the experimental results with the three H/D ratios, 1029, 1544, and 1802 discs with a diameter of 1.5 mm were generated to model a specimen with a diameter of 100 mm. The boundaries of the DSS models consisted of top and bottom walls and two side walls. Although some researchers (*e.g.*, Wijewickreme *et al*. 2013) have suggested increasing the friction coefficient on the top and bottom walls by 10 fold to reduce slippage, the same normal and shear stiffness parameters were assigned for all contact points between walls and balls for consistency.

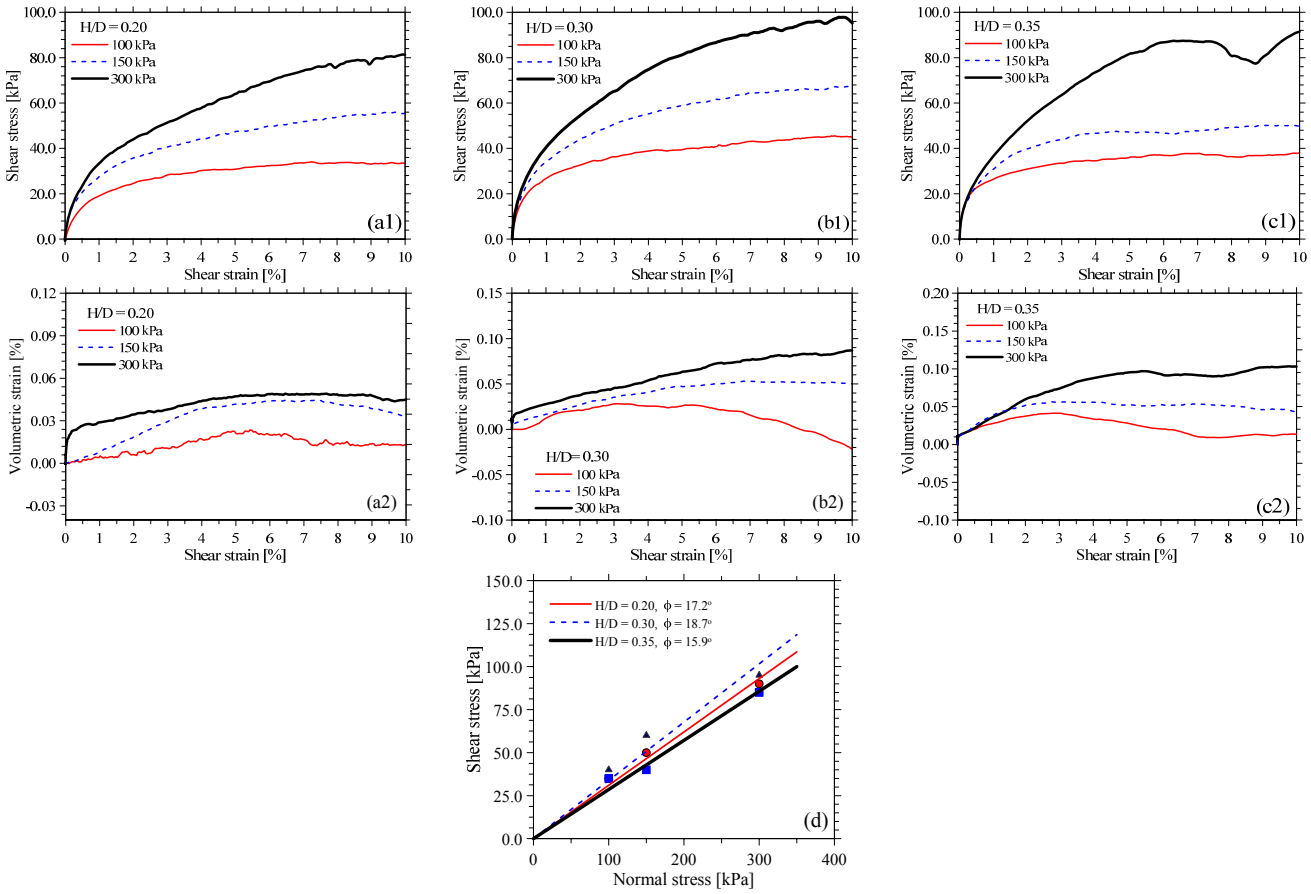

Fig. 3 DSS testing results for uniform steel balls: (a) H/D = 0.20, (b) H/D = 0.30 (c) H/D = 0.35, and (d) Mohr-Coulomb failure envelopes

The boundary conditions for the NGI- and Cambridge-type DSS configurations, denoted as NGI-DEM and CAM-DEM, respectively, were applied as shown in Fig. 4. For both configurations, the top wall is horizontally fixed and the bottom wall moves horizontally. For the NGI-DEM model, pairs of 2 mm vertical walls at the two vertical wall positions were employed to simulate layers of the stacked rings. At the same level, two stacked rings moved at the same horizontal velocity to maintain a constant cross section area for the Ko condition. Consecutive pairs of walls were employed to simulate the stacked rings of providing lateral constrains on the particle assembly. With the assumption that there is no friction between adjacent stacked rings and that the rings can move independently from each other, various horizontal velocities were applied to each stacked ring to shear the specimen under various deformation shapes. An idealized shearing mode with linearly varied horizontal velocity is shown in Fig. 4(a). For the CAM-DEM model, rigid side walls with rotational joints on the top and bottom walls were used to provide the lateral support. During the shearing phase, a constant spin rate of 10^{-8} rad/cycle was applied at the two rotation joints on the top wall, as shown in Fig. 4(b). To simulate the constant vertical stress condition during shearing, the top wall was allowed to move vertically and the vertical velocities of the top wall were controlled by a closed-loop servo mechanism. In the servo mechanism mode, the wall velocity is continuously adjusted according to the difference between the target and current stresses on the wall and set to zero when the difference is smaller than the tolerant value (Itasca 2008).

A linear contact model was employed to model the ball-to-ball and ball-to-wall contact conditions. The input parameters include ball geometry, material properties, contact constants, and numerical parameters. The geometry and material properties are directly assigned for round steel balls. The contact constants, including the normal and shear stiffness and coefficient of friction, are major input parameters that affect the micro- and macroscopic responses. Although advanced contact models have been proposed, the contact properties are too complicated and difficult to be employed. To focus on research subjects related to macroscopic size and boundary effects and simplify the simulation, a linear contact model and slip model were employed in the DEM simulation.

The micro mechanical properties of individual discs or contacts in DEM, including friction coefficient and normal and shear stiffness are not directly corresponded to macro properties (Seyferth and Henk 2005). Consequently, parametric studies were performed to investigate the effects of particulate contact stiffness on the macroscopic stress-strain relationships. The normal contact stiffness (k_n), shear contact stiffness (k_s) indicate the normal and shear components of inter-particle force and displacement. Yimsiri and Soga (2000) suggested that the normal stiffness constant is 2.5 times of the shear one. The slip model limits the maximum contact shear force with the friction coefficient. The friction coefficients in this study ranges from 0.2 to 0.30 according to the fitting results of the physical element tests. Same contact parameters are assigned for the contacts between particles and walls. Parametric study on the friction coefficient of the wall and stiffness constants shows that these wall parameters have minor effects on the macro responses. The contact parameters that best fit the physical test results are summarized in Table 1.

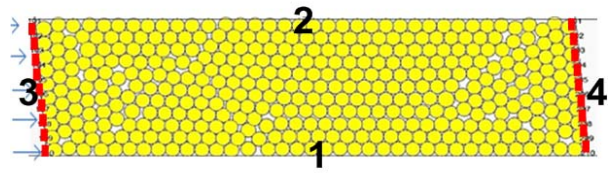

(a) NGI-DEM model

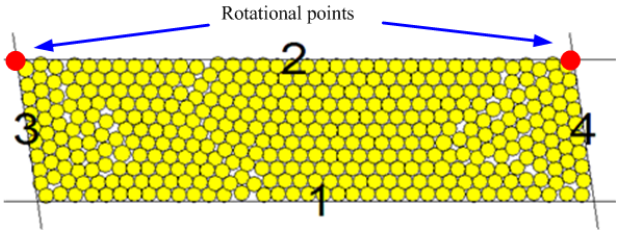

(b) CAM-DEM model

Fig. 4 NGI- and CAM- DEM models

Table 1 DEM Model parameters

Parameters	Balls	Wall (Stack ring)
Radius of ball r, (mm)	0.75	
Density, γ (Mg/m^3)	7.85	
Normal stiffness, k_n, (kN/m)	5.0×10^7	5.0×10^7
Shear stiffness, k_s (kN/m)	2.0×10^7	2.0×10^7
Damping ratio	0.70	0.70
Coefficient of friction, μ	0.2 ~ 0.3	0.2 ~ 0.3

3.2 Verification with Experiment Results

Using the NGI-DEM model shown in Fig. 4(a) and the input parameters listed in Table 1, the DEM macroscopic results with the testing data of steel balls are presented in Figs. 5(a) ~ 5(c) for H/D ratios of 0.20, 0.30, and 0.35, respectively. In the DEM results, the volumetric strain is calculated from the movement of the top wall, which is an average response on specimen, divided by the original height of the model and the compression is positive. Comparisons between the physical and NGI-DEM results show that the NGI-DEM can adequately simulate the stress-dependent, shear stress-strain curves at various H/D ratios. Although the volumetric responses are not as good as the shear stress-strain curves due to the difference in void volume calculations between the 2D-disc and 3D-ball packing, the DEM results show the trend of the granular system transforming from dilative to contractive responses with increasing vertical stress. Because the boundary and size effects are mainly related to shear-stress-related properties, the shear-induced dilative responses are excluded in the following discussions.

The effects of boundary conditions on the macroscopic stress-strain relationship are investigated using the calibrated set of model parameters on the two types of wall configurations. The CAM-DSS configuration is modeled with the CAM-DEM model in Fig. 4(b). Comparisons between the NGI-DEM and CAM-DEM models in terms of the stress-strain responses are shown in Fig. 6 for the three H/D ratios. The results show good agreement of the shear stress between NGI-DSS and CAM-DSS and the differences in the two configurations are insignificant. Comparisons of microscopic behaviors are presented later.

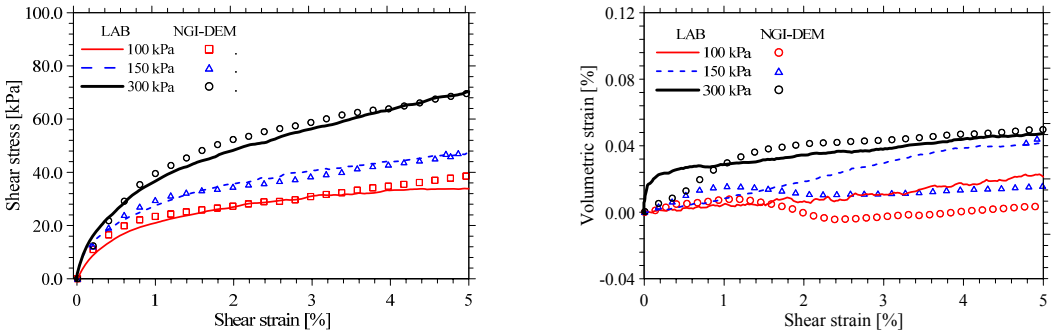

(a) $H/D = 0.20$

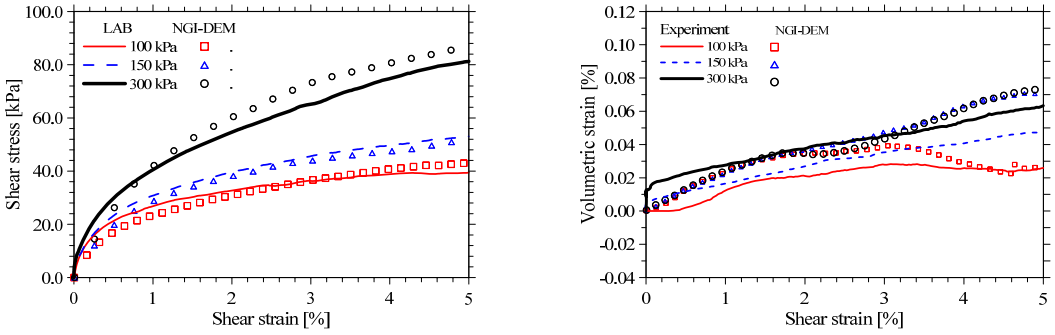

(b) $H/D = 0.30$

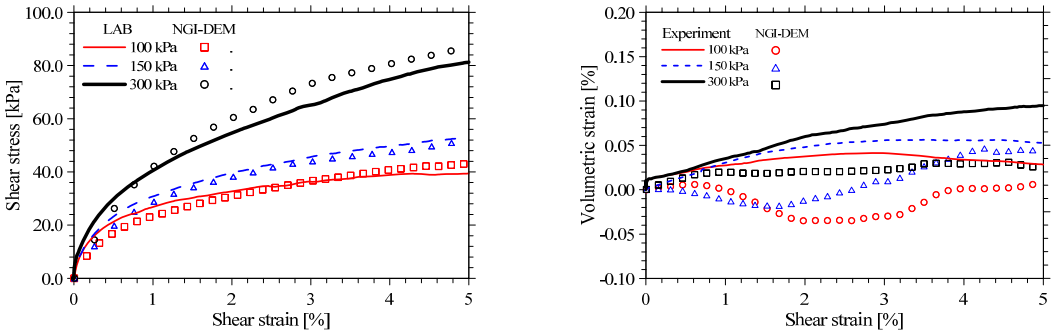

(c) $H/D = 0.35$

Fig. 5 Comparisons of experimental and DEM results

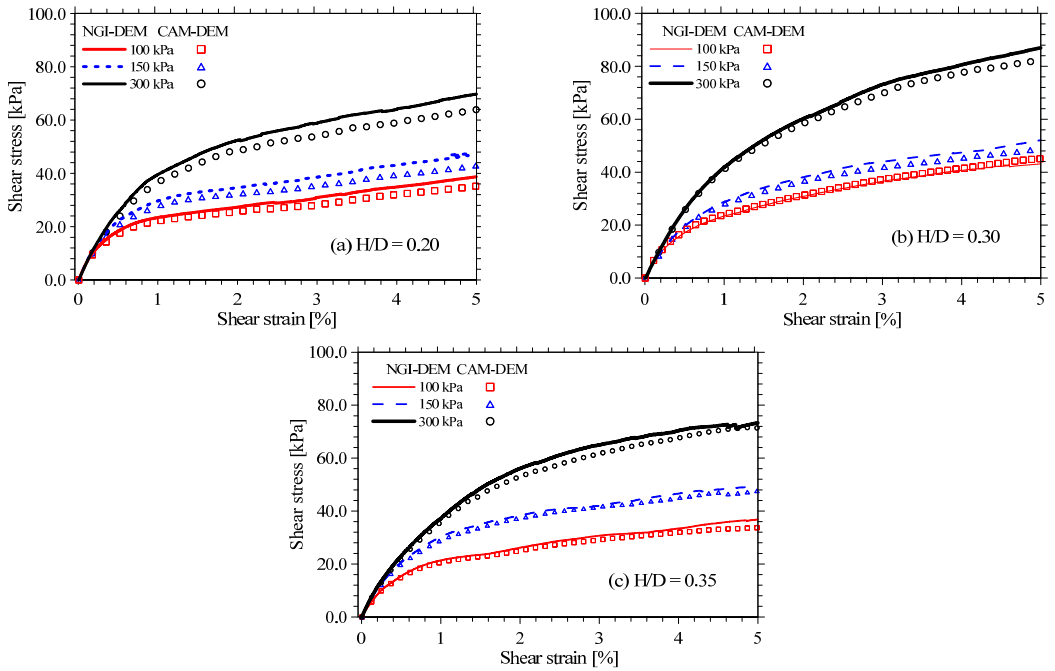

Fig. 6 Comparisons between NGI- and Cambridge-type DSS configurations

Another concern in NGI-DSS testing is the deformation shape of the vertical sides. In general, the vertical sides are generally assumed to have a linear shape and this shape is maintained throughout the shearing process. Unlike the CAM-DSS design, the NGI-DSS allows the lateral confinements to deform in different shapes other than the linear one. Three patterns of horizontal velocity profiles, namely linear, semi-parabolic, and ex-parabolic shapes, were applied to the NGI-DEM model for a specimen with a diameter of 100 mm and a height of 30 mm under a 300 kPa vertical stress. The macroscopic stress-strain relationships of the three deformation shapes along with the corresponding steel ball results are shown in Fig. 7. The results reveal that curved deformation shapes induce smaller shear stress at a given strain level and that the experimental curve becomes closer to the curved shapes with increasing strain level. The results imply that the curved deformation shapes might be more representative for the NGI-DSS test at large strain levels. Nevertheless, the percentage errors of induced shear stresses at 5% of the shear strain are less than 10% compared to the experiment results.

4. EVALUATION OF BOUNDARY AND SIZE EFFECTS IN DSS

4.1 Boundary Effects in DSS

The non-uniform distribution of stresses near specimen boundaries, which is generally referred as, boundary effect, is a major concern in DSS testing. Boundary effects had been evaluated using the finite element method based on continuum mechanics (*e.g.*, Lucks *et al*. 1972; Wright *et al.* 1978; Airey and Wood 1987). The results of these studies are significantly affected by selections of mesh size, constitutive laws of soils, and interface behaviors that describe the interactions between the soil and boundaries. DEM simulation is an alternative method for investigating this issue because no specific constitutive law or interface model is required. The calibrated DEM models are used to quantitatively evaluate the boundary effects.

In continua mechanics, boundary effects induce stress concentration near the boundaries. In DEM simulation, the stress distribution can be approximated as force chains, which represent the distribution of contact forces among particles. When a granular system is subjected to external loads, the loads are transmitted through a network of inter-particle contact forces (force chains). Thornton and Barnes (1986) called the force chains that transmitted the external loads by strong force network, which is the key microscopic feature of load transfer in a granular system. The particles that are not involved in the strong force network are called weak clusters, which have small loads at the inter-particle contact points (Radjai *et al.* 1996). The force chains of the NGI-DEM model with H/D = 0.30 and a vertical stress of 300 kPa at three strain levels are shown in Fig. 8, in which the thickness of the lines is proportional to the force magnitude.

The strong force network after the balance of the applied vertical stress is shown in Fig. 8(a). The weak clusters mostly exist near the two vertical walls; the spatial variation of the weak clusters becomes insignificant as the shear strain level increases (Figs. 8(b) ~ 8(c)). The core zone of the model is subjected to a relatively uniform contact force field and force chains in the core zone become more horizontally oriented as the shear strain level increases. The distribution of shear contact forces is shown in Fig. 9, in which a positive sign convention is toward the right direction. It shows that the majority of the model is subjected to a uniform shear contact force.

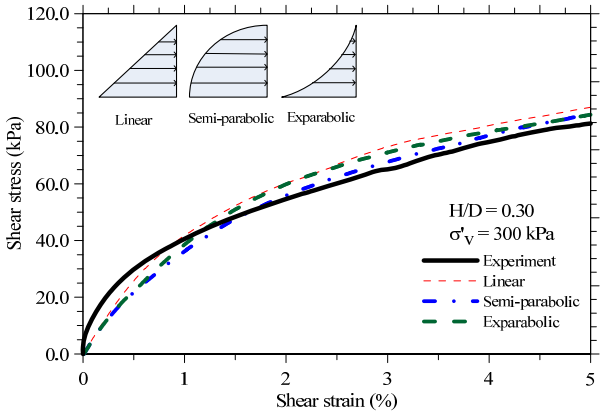

Fig. 7 Effects of deformation shape for NGI DSS

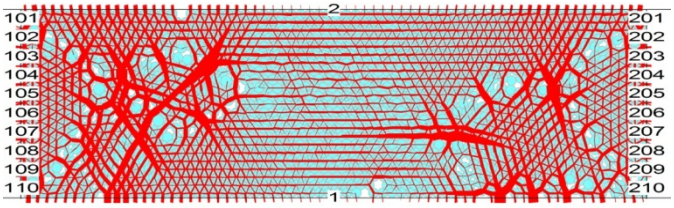

(a) γ = 0%

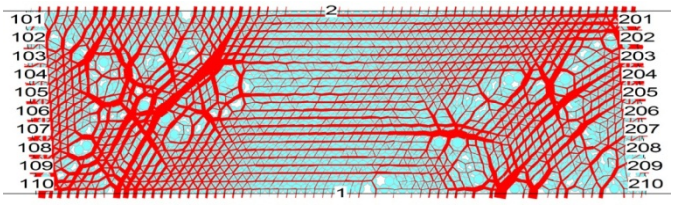

(b) γ = 5%

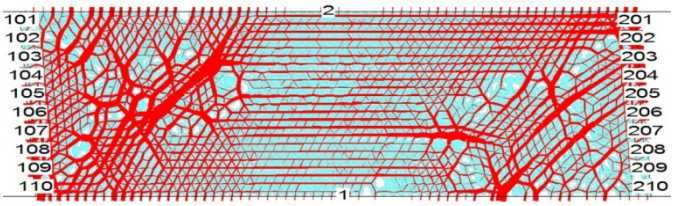

(c) γ = 8%

Fig. 8 Force chains of NGI-DEM with H/D = 0.30 and vertical stress of 300 kPa

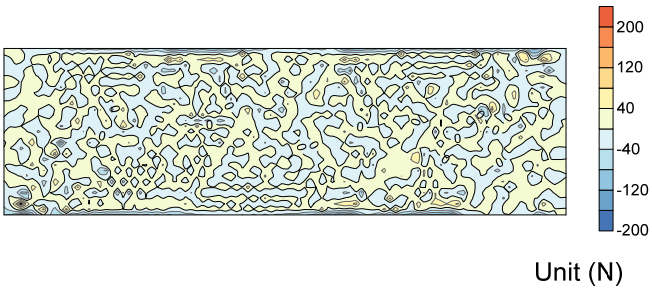

Fig. 9 Distribution of shear contact force in NGI-DEM model

The boundary effects for NGI-DEM and CAM-DEM models are presented in Fig. 10 in terms of the spatial variations of particle horizontal displacement. The results show that the differences in particle displacement field between the two configurations are small. In an idealized continuum, the horizontal dis-

placement should vary linearly along the vertical direction for strain-controlled testing with a fixed top cap. However, this trend only appears in the narrow zone near the two vertical boundaries (Fig. 10(a)). In the core zone of the model, a relatively uniform distribution of particle horizontal displacements was observed. The results disagree with the continuum mechanics framework. Furthermore, the small gradient of horizontal displacement implies that the local shear strain is small in the core zone. The spatial variation of particle displacement shows that the local shear strain level in the core zone is small and uniform and significant shear strain only developed in the four corners of the model. This can also be found from the stress vector of measurement circles. The core zone with uniform force chains and displacement field is about 60 to 70% of the total area of the model, which is consistent with the previous 3D finite element analysis by Lucks *et al*. (1972).

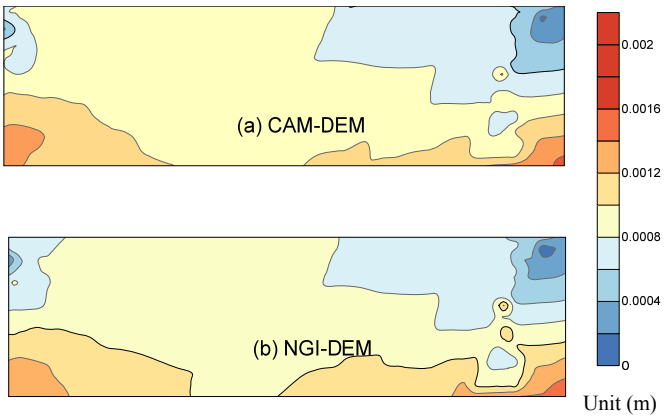

Fig. 10 Comparison of particle displacement between NGI-DEM and CAM-DEM models

4.2 DSS Specimen Size Effects

Previous studies (*e.g.*, Shen *et al*. 1978; Amer *et al*. 1987) have shown that the deviation of induced shear strain near the specimen boundaries decreased with decreasing H/D ratio. To investigate the specimen size effect on idealized granular assemblies, simulations of specimens with various diameters and a constant height were conducted. Three NGI-DEM models, with H/D ratios of 0.20, 0.30, and 0.40, respectively, were sheared to 8% of the shear strain under a vertical stress of 300 kPa. The distributions of particle normal contact force and horizontal displacement for the three H/D ratios at 8% of the shear strain are shown in Fig. 11. The distributions of contact shear force for different H/D ratios are not presented because the contact shear force at a contact point induces a rotation of particles. The difference in distribution of contact shear force for different H/D ratios is insignificant due to uniform rotation field induced during the shearing process.

The spatial variation of particle horizontal displacement (Fig. 11(a)) reveals that the displacement gradients near the two side walls are significantly higher than those in the core zone and that the displacement gradient in the core zone decreases significantly with decreasing H/D ratio. Because the deviation in the displacement gradient indicates a different shear strain field in the specimen, the horizontal displacement distribution reveals that the area percentage of uniform shear strain increases with decreasing H/D ratio. The contact force distributions in a particle system are related to the magnitude of the stress field in a continuum system. A uniform distribution of contact forces generally represents a relatively uniform stress field. However, the stresses in a continuum are different from the contact forces due to the directions of normal and shear stresses in a continuum element being different from the normal and shear directions at a contact point. Fig. 11(b) shows that the gradient variations of normal contact force is similar to those of horizontal displacement, with higher gradients near the vertical walls than those in the core zone, and that the area ratio of uniform normal contact forces increases with decreasing H/D ratio. The DEM simulations for different H/D ratios agree with previous experimental findings (*e.g.*, Shen *et al.* 1978; Amer *et al*. 1987) that showed that the uniformity of stress distribution increases with decreasing H/D ratio.

4.3 Effects of Maximum Diameter of Particles on DSS Test

Physical experimental studies show that the frictional angle of granular soils decreases as the maximum particle size (d_{max}) increases in drained, triaxial tests (Kirkpatrick 1965; Marachi *et al.* 1972). For a simple shear test, the d_{max} affects the width of the shear band. To reduce the inconsistency of results in a DSS test from d_{max}, ASTM D6528 requires that the height of specimens must be at least 10 times of the maximum particle size. The effects of specimen size are more important for testing gravelly soils due to the existence of large particles.

To investigate the effects of d_{max} on DSS testing results, a series of NGI-DEM simulations using calibrated model parameters with various values of d_{max} were conducted. Particle assemblies with a uniform distribution of particle sizes were generated by assigning a minimum radius of 0.075 mm and various maximum radii. The results for specimens with a height of 30 mm and H/D ratios of 0.2, 0.3, and 0.4 are shown in Fig. 12. The results show that d_{max} affects both the initial modulus and the shear strength when the value of H/d_{max} is smaller than a threshold value around 7 and that the stress-strain curves with different d_{max} values merge when d_{max} is decreased for a given H/D ratio. Because the ratio between the specimen height to the maximum particle size (H/d_{max}) is the number of stacked particle layers involved during shearing, the H/d_{max} ratio is related to the thickness of the shear band. Oda and Kazama (1998) revealed that the thickness of the shear band is 7 to 8 times the mean particle size for angular, granular soils and that particles outside the shear band do not provide macroscopic resistance against shearing. In cases in which the specimen height is smaller than the thickness of the shear band, the H/d_{max} value decreases or the number of sheared layers decreases as d_{max} increases, resulting in a reduction in resistance against shearing, as shown in Fig. 12. In contrast, for cases in which the specimen height is greater than the thickness of the shear band, the macroscopic resistance will not increase as the specimen height increases.

The relationships among H/D ratio, shear stress at 8% of the shear strain level, and H/d_{max} are shown in Fig. 13. The results reveal that there is a consistent shear resistance when the H/d_{max} value is no less than 7, regardless of the H/D ratio. For specimens with an H/d_{max} value of less than 7, the shear resistance is underestimated. In addition, the difference of shear resistance for different H/D ratios decreases with increasing H/D ratio. These results provide criteria for determining the specimen size of granular soils for consistent DSS results.

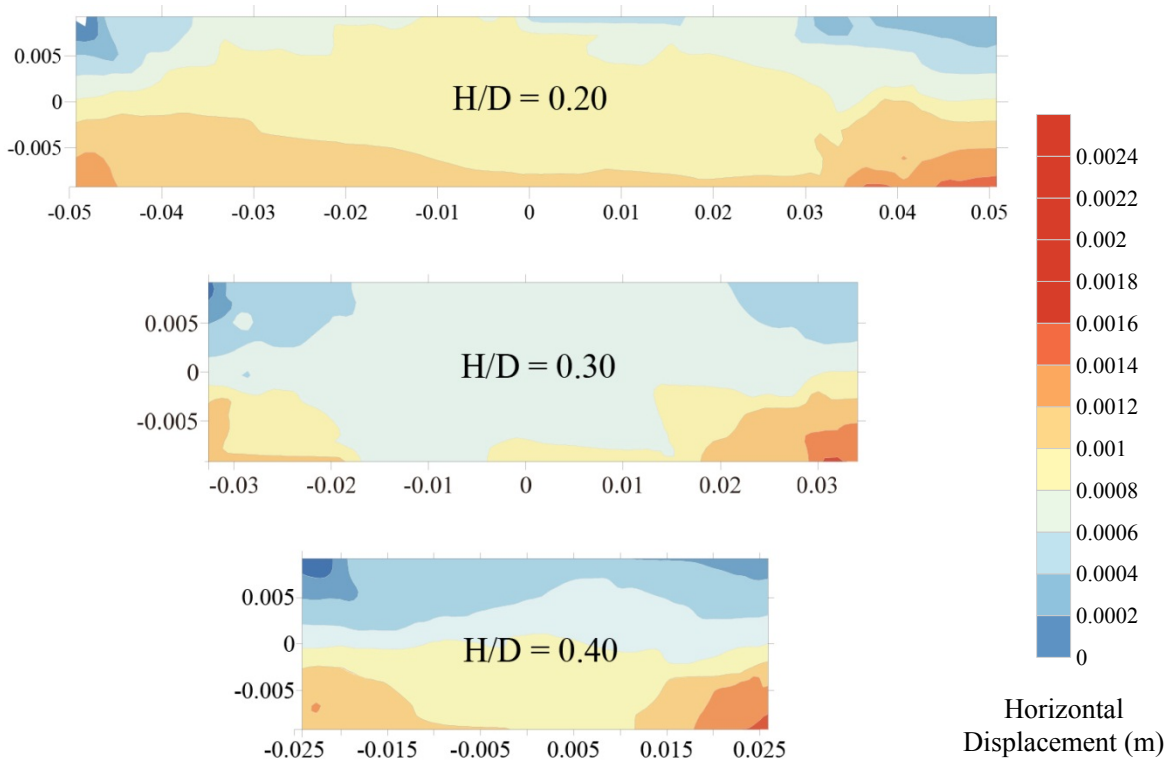

(a) Particle horizontal displacement

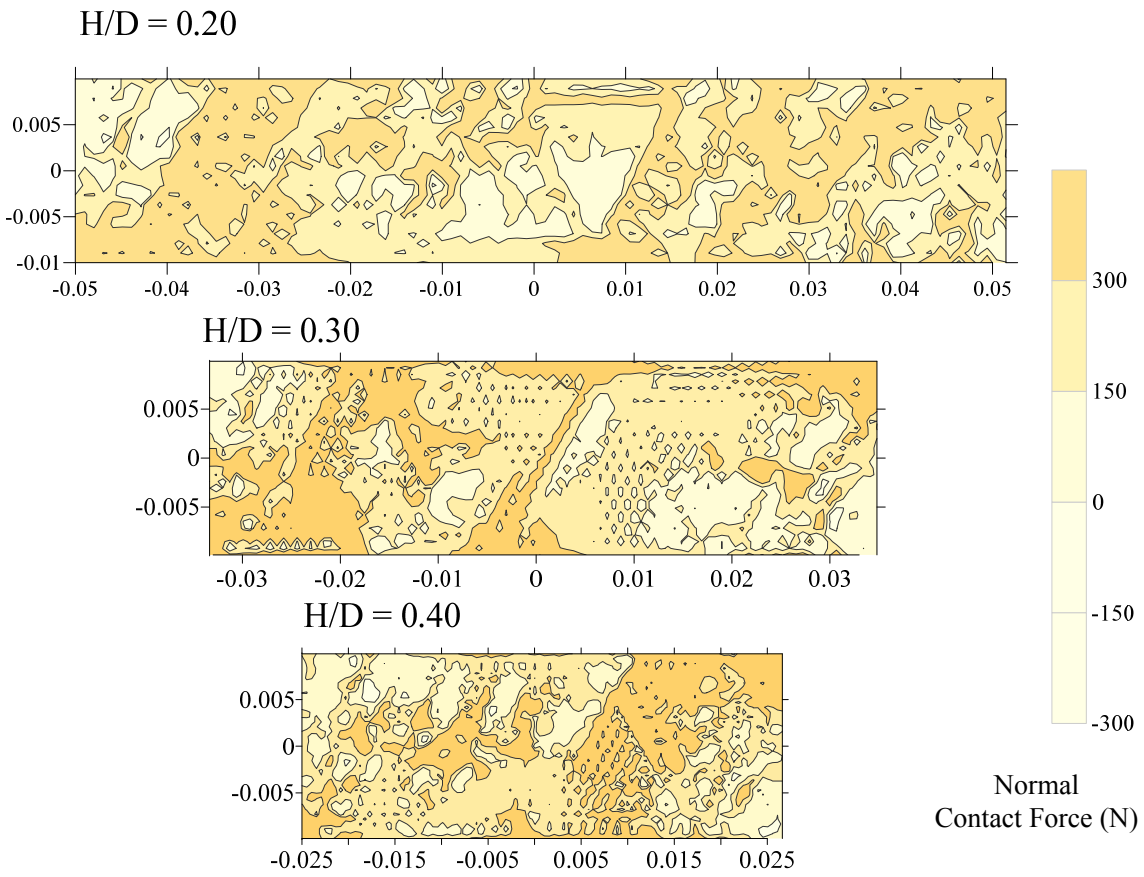

(b) Particle normal force

Fig. 11 DEM results for various *H*/*D* ratios

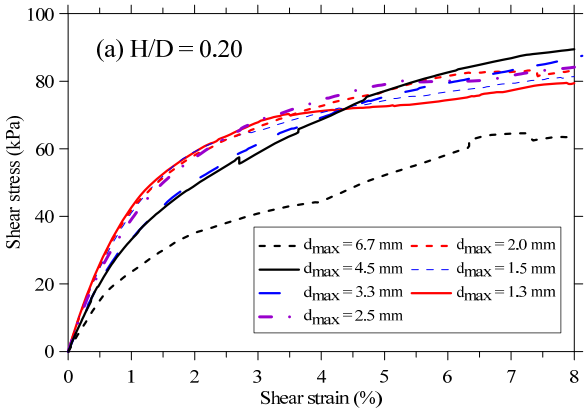

(a) $H/D = 0.2$

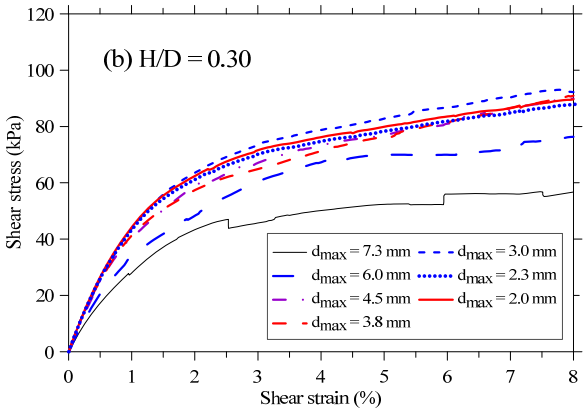

(b) $H/D = 0.3$

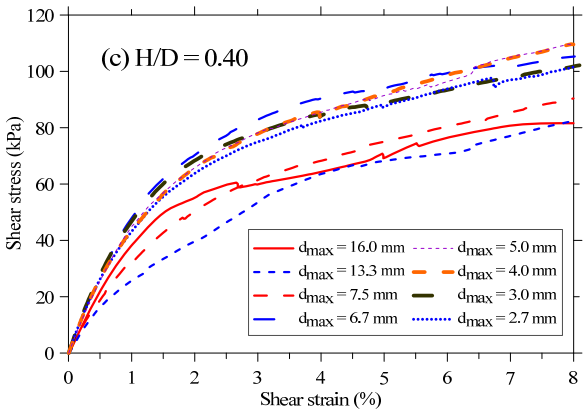

(c) $H/D = 0.4$

Fig. 12 Stress-strain curves for various d_{max} values

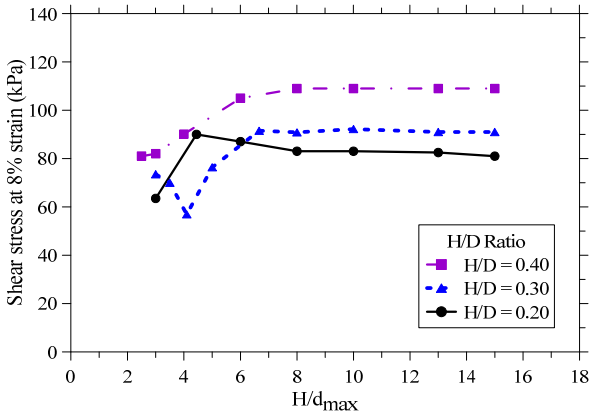

Fig. 13 Combined effects of H/D ratio and d_{max} on shear resistance

5. CONCLUSIONS

To determine the specimen size for DSS testing of gravelly soils, a series of DEM simulations were conducted to investigate the boundary and size effects for NGI- and Cambridge-type DSS configurations. The DEM models were calibrated using DSS data of uniform steel balls. The findings are summarized as followings:

1. The boundary effects can be reduced effectively by reducing the H/D value.
2. The core zone in DEM models of direct simple shear has uniform force chains and displacement field is about 60 to 70% of the total area of the model for H/D value ranging from 0.2 to 0.4.
3. The difference in boundary effects is insignificant between NGI- and Cambridge-type DSS.
4. A consistent shear resistance is available when the ratio of the specimen height to the maximum particle size (H/d_{max}) is no less than 7, regardless of the H/D value.

ACKNOWLEDGEMENTS

This study was supported by the Ministry of Science and Technology, Taiwan, under grant NSC 100-2625-M-006-008-MY3, which is gratefully acknowledged. Any opinions, findings, and conclusions or recommendations expressed in this material are those of the authors, and do not necessarily reflect the views of the Ministry of Science and Technology, Taiwan.

REFERENCES

Airey, D.W. and Wood, D.M. (1987). "An evaluation of direct simple shear tests on clay." *Géotechnique*, **37**(1), 25–35.

Amer, M.I., Kovacs, W.D., and Aggour, M.S. (1987). "Cyclic simple shear size effects." *Journal of Geotechnical Engineering*, **113**(7), 693–707.

Bjerrum, L. and Landva, A. (1966). "Direct simple-shear tests on a Norwegian quick clay." *Géotechnique*, **16**(1), 1–20.

Budhu, M. (1984). "Nonuniformities imposed by simple shear apparatus." *Canadian Geotechnical Journal*, **21**(1), 125–137.

Budhu, M. and Britto, A. (1987). "Numerical analysis of soils in simple shear devices." *Soils and Foundations*, **27**(2), 31–41.

Chang, W.J., Chang, C.W., and Zeng, J.K. (2014). "Liquefaction characteristics of gap-graded gravelly soils in K0 condition." *Soil Dynamics and Earthquake Engineering*, **56**, 74–85.

Cui, L. and O'Sullivan, C. (2006). "Exploring the macro-and micro-scale response of an idealised granular material in the direct shear apparatus." *Geotechnique*, **56**(7), 455–468.

Cundall, P.A. and Strack, O.D. (1979). "A discrete numerical model for granular assemblies." *Géotechnique*, **29**, 47–65.

Dabeet, A., Wijewickreme, D., and Byrne, P. (2015). "Evaluation of stress strain non-uniformities in the laboratory direct simple shear test specimens using 3D discrete element analysis." *Geomechanics and Geoengineering*, **10**(4), 249–260.

Doherty, J. and Fahey, M. (2011). "Three-dimensional finite element analysis of the direct simple shear test." *Computers and Geotechnics*, **38**(7), 917–924.

Dounias, G.T. and Potts, D.M. (1993). "Numerical analysis of drained direct and simple shear tests." *Journal of Geotechnical Engineering*, **119**(12), 1870–1891.

Itasca Consulting Group, Inc. (2008). *PFC2D Particle Flow Code in Two Dimensions, Ver.4.0 User's Guide*. Minneapolis, MN: Itasica.

Kirkpatrick, W.M. (1965). "Effects of grain size and grading on the shearing behaviour of granular Materials." *Proceedings of 6th International Conference on Soil Mechanics and Foundation Engineering*, **1**, 273–277.

Kjellman, W. (1951). "Testing the shear strength of clay in Sweden." *Géotechnique*, **2**(3), 225–232.

Kishida, H. and Uesugi, M. (1987). "Tests of the interface between sand and steel in the simple shear apparatus." *Geotechnique*, **37**(1), 45–52.

Kozicki, J. and Donzé, F. V. (2008). "A new open-source software developed for numerical simulations using discrete modeling methods." *Computer Methods in Applied Mechanics and Engineering*, **197**(49-50), 4429–4443.

Ladd, C.C. and Foott, R. (1974). "New design procedure for stability of soft clays." *Journal of the Geotechnical Engineering Division*, **100**(7), 763–786.

Lucks, A.S., Christian, J.T., Brandow, G.E., and Hřeg, K. (1972). "Stress conditions in NGI simple shear test." *Journal of the Soil Mechanics and Foundations Division*, **98**(1), 155–160.

Marachi, N.D., Chan, C.K., and Seed, H.B. (1972). "Evaluation of properties of rockfill materials." *Journal of Soil Mechanics & Foundations Division*, **97**(1), 95–114.

Oda, M. and Kazama, H. (1998). "Microstructure of shear bands and its relation to the mechanisms of dilatancy and failure of dense granular soils." *Géotechnique*, **48**(4), 465–481.

Prevost, J.H. and Høeg, K. (1976). "Reanalysis of simple shear soil testing." *Canadian Geotechnical Journal*, **13**(4), 418–429.

Radjai, F., Jean, M., Moreau, J.J., and Roux, S. (1996). "Force distributions in dense two-dimensional granular systems." *Physical Review Letters*, **77**(2), 274–277.

Roscoe, K.H. (1953). "An apparatus for the application of simple shear to soil samples." *Proceedings of Third International Conference on Soil Mechanics and Foundation Engineering*, **1**, 186–191.

Seyferth, M. and Henk, A. (2006). "A numerical sandbox: high-resolution distinct element models of halfgraben formation." *International Journal of Earth Sciences*, **95**(2), 189–203.

Shen, C.K., Sadigh, K., and Herrmann, L.R. (1978). "An analysis of NGI simple shear apparatus for cyclic soil testing." *ASTM Special Technical Publication*, **654**, 148–162.

Thornton, C., (2000). "Numerical simulations of deviatoric shear deformation of granular media." *Géotechnique*, **50**(1), 43–53.

Thornton, C. and Barnes, D.J. (1986). "Computer simulated deformation of compact granular assemblies." *Acta Mechanica*, **64**(1-2), 45–61.

Wang, J. and Gutierrez, M. (2010). "Discrete element simulations of direct shear specimen scale effects." *Géotechnique*, **60**(5), 395–409.

Wijewickreme, D., Dabeet, A., and Byrne, P. (2013). "Some observations on the state of stress in the direct Simple shear test using 3D discrete element analysis." *ASTM Geotechnical Testing Journal*, **36**(2), 292–299.

Wright, D.K., Gilbert, P.A., and Saada, A.S. (1978). "Shear devices for determining dynamic soil properties." *Proceedings of ASCE Specialty Conference on Earthquake Engineering and Soil Dynamics*, **2**, 1056–1075.

Yimsiri, S. and Soga, K. (2000). "Micromechanics-based stress–strain behaviour of soils at small strains." *Géotechnique*, **50**(5), 559–571.

Zhao, X. and Evans, T. (2009). "Discrete simulations of laboratory loading conditions." *International Journal of Geomechanics*, **9**(4), 169–178.